J. Fluid Mech. (1975), *vol.* 70, *part* 1, *pp.* 179–205
Printed in Great Britain

On turbulence and noise of an axisymmetric shear flow

By A. MICHALKE
Institut für Thermo- und Fluiddynamik, Technische Universität, Berlin
AND H. V. FUCHS
DFVLR-Institut für Turbulenzforschung, Berlin

(Received 15 July 1974 and in revised form 18 November 1974)

The noise produced by mean flow–turbulence interaction of a circular subsonic jet is investigated theoretically, and expanded in azimuthal constituents of the turbulent pressure fluctuations. It is found that the low-order azimuthal constituents are the most efficient sound sources. On the basis of pressure correlation measurements, the azimuthal constituents are determined in a low Mach number jet. It is found that, in a range of Strouhal numbers between 0·2 and 1, the first three to four azimuthal constituents clearly dominate over the rest of the turbulent source quantity. A strictly axisymmetric ring vortex model for the coherent structure of the turbulence is, however, shown to be inappropriate.

1. Introduction

Despite the fact that numerous papers on jet noise have already been published, it is felt that this long-standing problem is a great way from being thoroughly understood, as far as the modelling of turbulence is concerned. The large-scale orderly structure of jet turbulence, found by Mollo-Christensen (1963) and explained by Crow & Champagne (1971) as being produced by an instability of the turbulent jet boundary layer, became the subject of a discussion as to how relevant the coherent part of the turbulence might be to the jet noise problem. It is clear that, if the coherent part of jet turbulence were to contribute essentially to the far-field of jet noise, several so far well-accepted assumptions, about jet turbulence and its effect on jet noise, would have to be re-examined.

A theoretical approach to the jet noise problem, which is most apt to take into account large-scale phenomena of jet turbulence, has been proposed by Michalke (1970, 1971). Starting from Lighthill's equation, the basic idea of that approach was to include symmetry conditions in a circular jet. By introducing cylindrical co-ordinates, the source term of the Lighthill equation was expanded with respect to the azimuthal angle. A Fourier transform with respect to time finally led to the conclusion that the axisymmetric and low-order azimuth-frequency components of the source term should be the most efficient sound sources in a circular jet.

It was another question, however, whether such components of turbulence exist in practice in a turbulent jet. Measurements of pressure fluctuations in jets by Lau, Fisher & Fuchs (1972) and by Fuchs (1972*b*) gave strong evidence for the

existence of axisymmetric, wavelike pressure components. But there was still the problem of how these pressure components could be related to Lighthill's source term and the far-field noise.

The objective of this paper is to describe the jet noise far field by means of the turbulent pressure fluctuations, and identify quantities of the turbulence that are the most closely related to the radiated noise. Furthermore, by experiments, the jet turbulence is investigated with respect to these quantities, in order to estimate their magnitude and relative importance for the radiated noise. It is not intended to calculate and measure in detail the far-field noise characteristics, however.

The theoretical part of this paper is restricted to that part of jet noise generated by the interaction of turbulence with the mean shear flow. Neglect of the so-called 'self-noise' produced by turbulence–turbulence interaction may be somewhat questionable, although many authors have proceeded in this way (cf. Lighthill 1954; Lilley 1958; Ribner 1962; Jones 1968; Pao & Lowson 1968). But it is felt that, at least in certain regions of the jet flow, and with respect to certain directions of noise radiation, the noise produced by the mean flow–turbulence interaction may be dominant.

For subsonic Mach numbers, the power spectral density of the far-field noise produced by mean flow–turbulence interaction is derived in § 2. It is essentially determined by the cross-spectral density $W_{p_1 p_2}$ of the turbulent pressure fluctuations. Following the scheme of Michalke (1972), $W_{p_1 p_2}$ is expanded in a Fourier series of azimuthal constituents $\tilde{W}_{12,m}$ in § 3, and introduced into the sound power spectrum. The importance of the various azimuthal constituents with respect to the sound power spectrum is discussed in § 4. The measuring of pressure fluctuations and their filtered space correlations is described in § 5, while § 6 deals with the evaluation of circumferential correlations with respect to the azimuthal constituents. Results of measurements at low Mach numbers are presented in § 7. These show the importance of the low-order azimuthal constituents $\tilde{W}_{12,m}$ in the Strouhal number range $0{\cdot}2 \leqslant St \leqslant 1$ for the circular jet and $x/D \leqslant 10$. A final discussion of the experimental results, and their importance for the theoretically derived far-field noise, is given in § 8. A more elaborate description of the present investigation can be found in Michalke & Fuchs (1974).

2. Theory of sound produced by mean flow–turbulence interaction

Our theoretical approach to the jet noise problem is based on the Lighthill equation

$$\frac{1}{a_0^2}\frac{\partial^2 p}{\partial t^2} - \frac{\partial^2 p}{\partial x_i^2} = \frac{\partial^2}{\partial x_i \partial x_j}(\rho c_i c_j - \tau_{ij}) + \frac{\partial^2}{\partial t^2}\left[\frac{p}{a_0^2} - \rho\right]. \tag{2.1}$$

Here a_0 is the constant speed of sound in the fluid at rest surrounding the jet flow; p, ρ and c_i are the pressure, density and velocity vector in Cartesian co-ordinates x_i, respectively. In the following, we neglect the viscous stress tensor τ_{ij} and the last term in (2.1), which is only important when entropy and/or pressure fluctuations, in connexion with a mean temperature profile, are present in the jet flow. This approximation is justified for large Reynolds numbers, and for a jet

temperature equal to the ambient temperature at moderate subsonic Mach numbers.

The sound pressure p_s in a far-field approximation is then, according to Lighthill (1952),

$$p_s(x_i,t) = \frac{1}{4\pi\tilde{r}}\frac{x_i x_j}{\tilde{r}^2}\frac{1}{a_0^2}\int_V dV\left[\frac{\partial^2}{\partial t^2}(\rho c_i c_j)\right]. \tag{2.2}$$

The brackets [ ] indicate that the expression is to be evaluated at the retarded time

$$t_r = t - \frac{\tilde{r}}{a_0} + \frac{x_i y_i}{a_0 \tilde{r}}. \tag{2.3}$$

y_i denote the Cartesian co-ordinates of the source points; and dV is the volume element of the source volume V and $\tilde{r} = |x_i|$.

With the index r indicating a vector component in the direction of x_i, (2.2) can alternatively be written as

$$p_s(x_i,t) = \frac{1}{4\pi\tilde{r}}\frac{1}{a_0^2}\int_V dV\left[\frac{\partial^2}{\partial t^2}(\rho c_r^2)\right]. \tag{2.4}$$

It is clear that the far-field sound pressure p_s can be calculated, if the source function in the integrand of (2.2) is known. This assumption is the basis of Lighthill's theory. It implies that the required flow quantities can be measured and/or described analytically. But this is the critical point, since a sufficiently accurate measurement of the tensor quantity $\rho c_i c_j$, or its correlation function, is a formidable task. With respect to the mean flow–turbulence interaction term of sound pressure (the subject here), the source function can be expressed by the pressure fluctuations, which have the advantage of being a scalar quantity.

By means of the inviscid equation of motion and the continuity equation, another equivalent form of the solution (2.4) can be derived. As shown in the appendix, for a local Mach number component in the x_i direction

$$M_r = \frac{x_i}{\tilde{r}}\frac{c_i}{a_0} = \frac{c_r}{a_0} < 1, \tag{2.5}$$

(2.4) can be written as

$$p_s(x_i,t) = \frac{1}{4\pi\tilde{r}}\frac{1}{a_0^2}\int_V dV\left[2\frac{\partial}{\partial t}\left(\frac{p}{(1-M_r)^3}\frac{\partial c_r}{\partial y_r}\right) + \frac{1}{a_0}\frac{\partial^2}{\partial t^2}\left(\frac{pc_r(2-M_r)}{(1-M_r)^2}\right)\right]. \tag{2.6}$$

$\partial/\partial y_r$ is the gradient in the x_i direction.

When the velocity vector c_i is split into a mean $\bar{c}_i$ and a fluctuating part c_i' (note $p = p'$), one obtains in (2.6) a mean flow–turbulence interaction term $p_{s,\mathrm{MT}}$ (or briefly, p_{MT}), which is generated by the turbulent pressure fluctuations p' alone, and a turbulence–turbulence interaction term $p_{s,\mathrm{TT}}$, which is generated by, at least, products of turbulent fluctuations.

In the following, of the p_{MT} terms we shall deal with only

$$p_{\mathrm{MT}}(x_i,t) = \frac{1}{4\pi\tilde{r}}\frac{1}{a_0^2}\int_V dV\left\{\frac{2}{(1-\bar{M}_r)^3}\frac{\partial \bar{c}_r}{\partial y_r}\left[\frac{\partial p'}{\partial t}\right] + \frac{\bar{M}_r(2-\bar{M}_r)}{(1-\bar{M}_r)^2}\left[\frac{\partial^2 p'}{\partial t^2}\right]\right\}. \tag{2.7}$$

For $\bar{M}_r \to 0$ (2.7) is usually denoted as the 'shear-noise' term, which was first discussed by Lighthill (1954). The last term of (2.7) corresponds to one neglected in that paper, using the argument that it "represents an octupole field and must be expected to radiate relatively little sound, especially at lower Mach numbers". This is, in fact, evident from (2.7). However, because the second term is proportional to the second time derivative of the pressure, in contrast to the first time derivative of the first term, the decisive parameter for the importance of both terms in (2.7) is (besides the factors containing different mean flow quantities) the product of Mach number and a characteristic frequency (Strouhal number).

In order to avoid confusion, it should be emphasized that, in (2.7), the integration over the source volume is with respect to a *fixed* frame of reference. The powers of $(1-\bar{M}_r)$ should therefore not be mistaken for convective amplification terms of the type $(1-M_c\cos\theta)^{-n}$, which are obtained when the turbulence is considered in a frame of reference moving with a convection Mach number M_c. The power spectral density W_{MT} of p_{MT} can be deduced from (2.7) by standard methods, via the autocorrelation R_{MT} and its Fourier transform, yielding

$$W_{\mathrm{MT}}(x_i) = \left(\frac{1}{4\pi\tilde{r}}\right)^2 \frac{\omega^2}{a_0^4} \int_V dV_1 \int_V dV_2 \{\hat{L}_1 L_2 W_{p_1 p_2} \exp\left[ik_i(y_{i2}-y_{i1})\right]\}. \tag{2.8}$$

Here L is a complex quantity, which depends on the mean flow quantities and on frequency in the following manner:

$$L = \frac{2}{(1-\bar{M}_r)^3}\frac{\partial \bar{c}_r}{\partial y_r} - ik\frac{2-\bar{M}_r}{(1-\bar{M}_r)^2}\bar{c}_r. \tag{2.9}$$

The superscript $\hat{}$ denotes the complex conjugate value. The local position in the source region at y_{i1} is denoted by the index 1, and the position at y_{i2} by the index 2. $W_{p_1 p_2}$ is the cross-spectral density of the turbulent pressure fluctuations p'. Furthermore, the wavenumber of sound and the wavenumber vector in the x_i direction are denoted by

$$k = \omega/a_0 = 2\pi f/a_0, \quad k_i = kx_i/\tilde{r}. \tag{2.10}$$

f is the frequency. The exponential term with imaginary argument in (2.8) takes the effect of retarded time into account or with other words, it is an acoustic interference function acting on the sound sources distributed in the jet. Only when the spatial extension of the 'effective' source distribution (defined by $|\hat{L}_1 L_2 W_{p_1 p_2}| \geqslant \epsilon$ for a sufficiently small ϵ) is small compared with the sound wavelength $2\pi/k$ can we treat the source distribution as 'acoustically compact', and neglect the acoustic interference. In order to evaluate (2.8), the mean velocity distribution $\bar{c}_i(y_i)$ and the cross-spectral density $W_{p_1 p_2}(y_{i1}, y_{i2})$ of the turbulent pressure fluctuations have to be known. But both quantities can be measured in a turbulent jet by means of hot-wire techniques, and by the pressure correlation techniques (cf. Fuchs 1972*a*, *b*).

3. Expansion of the source term

As proposed by Michalke (1970), it is appropriate for a circular jet to use cylindrical co-ordinates (x, r, ϕ) instead of the Cartesian co-ordinates y_i, where the x direction coincides with the jet axis. The Cartesian co-ordinates x_i of the

field point are conveniently replaced by polar co-ordinates $(\tilde{r}, \theta, \phi')$, where θ is the angle with respect to the jet axis.

The turbulent pressure fluctuations $p'(x, r, \phi, t)$ in the source region can then be expanded in a Fourier series with respect to the azimuthal angle ϕ (cf. Michalke 1972). This means that the turbulent fluctuations can be separated into axisymmetric and higher-order azimuthal components. Because of symmetry conditions in a circular jet, the cross-spectral density $W_{p_1 p_2}$ of the pressure fluctuations can depend only on $\Delta\phi = \phi_2 - \phi_1$, not on ϕ_2 and ϕ_1 separately. Additionally, $W_{p_1 p_2}$ must be a periodic function with respect to $\Delta\phi$. Therefore the cross-spectral density can be expanded in a Fourier series in $\Delta\phi$:

$$W_{p_1 p_2} = \sum_{m=-\infty}^{\infty} W_{12,m}(x_1, r_1, x_2, r_2) \exp(im\Delta\phi). \tag{3.1}$$

$W_{12,m}$ are the complex Fourier coefficients. It may be noted that each $W_{12,m}$ is determined solely by the corresponding mth azimuthal constituent of the pressure itself.

The mean velocity field of a circular jet without swirl consists of an axial velocity component $\bar{u}(x, r)$ and a radial component $\bar{v}(x, r)$. Hence the mean velocity component in the x_i direction is

$$\bar{c}_r = \frac{x_i}{\tilde{r}} \bar{c}_i = \bar{u} \cos\theta + \bar{v} \sin\theta \cos\chi, \tag{3.2}$$

where $$\chi = \phi - \phi'.$$

Furthermore, we find

$$\frac{\partial \bar{c}_r}{\partial y_r} = \cos^2\theta \frac{\partial \bar{u}}{\partial x} + \tfrac{1}{2} \sin 2\theta \cos\chi \left(\frac{\partial \bar{u}}{\partial r} + \frac{\partial \bar{v}}{\partial x} \right) + \sin^2\theta \left(\cos^2\chi \frac{\partial \bar{v}}{\partial r} + \sin^2\chi \frac{\bar{v}}{r} \right). \tag{3.3}$$

Let us denote the jet exit velocity by U_0 and the nozzle exit diameter by D, and normalize all velocities by U_0 and the co-ordinates x, r, $\tilde{r}$ by D. Then we have the dimensionless mean velocities

$$U = \bar{u}/U_0 \quad \text{and} \quad V = \bar{v}/U_0 \quad \text{with} \quad U \leqslant 1,$$

whereas for a jet flow $|V| \ll 1$ holds. Again, the dimensionless co-ordinates

$$X = x/D, \quad R = r/D \quad \text{and} \quad \tilde{R} = \tilde{r}/D$$

will be introduced.

Finally, we assume a jet Mach number $M = U_0/a_0 < 1$. Then from (3.2) it follows that approximately ($|V| \ll 1$)

$$1 - \bar{M}_r \approx 1 - U(X, R) M \cos\theta. \tag{3.4}$$

Using (3.2), (3.3) and the approximation (3.4), one obtains from (2.9), by a simple calculation,

$$L = \frac{U_0}{D} \sum_{n=0}^{2} A_n \cos(n\chi), \tag{3.5}$$

where

$$\left.\begin{aligned} A_0 &= \frac{1}{(1-UM\cos\theta)^3}\left[2\cos^2\theta\frac{\partial U}{\partial X}+\sin^2\theta\left(\frac{\partial V}{\partial R}+\frac{V}{R}\right)\right] \\ &\quad -ikD\cos\theta\frac{(2-UM\cos\theta)}{(1-UM\cos\theta)^2}U, \\ A_1 &= \frac{\sin 2\theta}{(1-UM\cos\theta)^3}\left[\frac{\partial U}{\partial R}+\frac{\partial V}{\partial X}\right]-ikD\sin\theta\frac{(2-UM\cos\theta)}{(1-UM\cos\theta)^2}V, \\ A_2 &= \frac{\sin^2\theta}{(1-UM\cos\theta)^3}\left[\frac{\partial V}{\partial R}-\frac{V}{R}\right]. \end{aligned}\right\} \tag{3.6}$$

Equation (2.10) yields

$$k_i(y_{i2}-y_{i1}) = -kD\{(X_2-X_1)\cos\theta+\sin\theta(R_2\cos\chi_2-R_1\cos\chi_1)\}. \tag{3.7}$$

The dimensionless frequency may be expressed by the Strouhal number $St = fD/U_0$, and is related to kD by

$$kD = 2\pi fD/a_0 = 2\pi StM. \tag{3.8}$$

Introducing (3.1), (3.5) and (3.7) into (2.8), the sound pressure power spectrum becomes, after integration with respect to χ_1 and χ_2,

$$W_{\mathrm{MT}}(\tilde{R},\theta) = \frac{M^4St^2}{4\tilde{R}^2}\sum_{m=-\infty}^{\infty}\int_{-\infty}^{\infty}dX_1\int_0^{\infty}dR_1R_1\int_{-\infty}^{\infty}dX_2\int_0^{\infty}dR_2R_2 \\ \times W_{12,m}(X_1,R_1,X_2,R_2)\,\hat{Z}_{m1}Z_{m2}\exp\{-ikD\cos\theta(X_2-X_1)\}. \tag{3.9}$$

The quantity Z_m is defined by

$$Z_m = (-i)^m\pi\{2A_0(X,R,\theta)\,J_m(\sigma)+iA_1(X,R,\theta)\,[J_{m-1}(\sigma)-J_{m+1}(\sigma)] \\ -A_2(X,R,\theta)\,[J_{m-2}(\sigma)+J_{m+2}(\sigma)]\}. \tag{3.10}$$

Here J_m is the Bessel function of order m and

$$\sigma = kD\sin\theta R. \tag{3.11}$$

It is easily seen from the behaviour of the Bessel functions that the product $\hat{Z}_{m1}Z_{m2}$ remains the same when m is replaced by $-m$. Hence the solution (3.9) can also be written as an infinite sum with only positive m:

$$W_{\mathrm{MT}}(\tilde{R},\theta) = \frac{M^4St^2}{4\tilde{R}^2}\sum_{m=0}^{\infty}\int_{-\infty}^{\infty}dX_1\int_0^{\infty}dR_1R_1\int_{-\infty}^{\infty}dX_2\int_0^{\infty}dR_2R_2 \\ \times\tilde{W}_{12,m}(X_1,R_1X_2,R_2)\,\hat{Z}_m(X_1,R_1,\theta)\,Z_m(X_2,R_2,\theta)\exp[-ikD\cos\theta(X_2-X_1)] \tag{3.12}$$

where

$$\left.\begin{aligned} \tilde{W}_{12,m} &= W_{12,m}+W_{12,-m} \quad \text{for} \quad m\geqslant 1, \\ \tilde{W}_{12,m} &= W_{12,m} \quad\quad\quad\quad\ \text{for} \quad m = 0. \end{aligned}\right\} \tag{3.13}$$

Up till now, we have not introduced any model of turbulence. But we can see, from (3.12), that the sound pressure power spectrum W_{MT} is built up from contributions of the individual azimuth-frequency components of the turbulent pressure. This is reasonable, but the important result is that each member of the

series is strongly weighted by the terms Z_m. According to (3.10) and (3.6), these terms contain (besides mean flow quantities) the Bessel functions J_m, $J_{m\pm1}$, $J_{m\pm2}$, which are independent of the flow quantities, but depend on m and on the argument σ defined by (3.11).

4. Discussion of the theoretical results

The expansion of turbulence into azimuthal constituents, introduced in § 3, leads to the result (3.12). It shows very clearly that two different interference mechanisms influence the sound radiation. The first one is the axial interference expressed by the exponential function with imaginary argument. This function is independent of m and therefore the same for all azimuthal constituents. The second mechanism is the radial interference expressed by the Bessel functions J_m, $J_{m\pm1}$, $J_{m\pm2}$ in (3.10), which depend on m and σ. Therefore, the influence of the radial interference is different for each azimuthal constituent. Owing to (3.11), the argument of the Bessel function is proportional to kD, (3.8), and $\sin\theta$. Owing to (3.6), the quantities A_0, A_1 and A_2 in (3.10) depend on θ, on kD and on the mean flow properties, but are independent of m. Therefore they can be assumed to be known. As function of the radial co-ordinate R, the quantities A_0, A_1 and A_2 vanish outside the jet, since the mean flow there tends to zero. Hence we can restrict the integration to, say, $(R_1, R_2) \leqslant R^*$. For a circular jet, we know from experiments that, in $0 \leqslant X \leqslant 12$, we have approximately $0{\cdot}5 \leqslant R^* \leqslant 2$. Hence, the upper bound for σ is $\sigma \leqslant \delta$, where

$$\delta = (kD\sin\theta)\,R^* = 2\pi StMR^*\sin\theta. \tag{4.1}$$

δ can be taken as a jet thickness parameter, since it is a measure of the acoustical thickness of the jet relative to the sound wavelength. As function of the jet angle θ, δ is a maximum for $\theta = 90°$ (i.e. normal to the jet axis), but δ is zero for both $\theta = 0°$ and 180° independent of kD. Hence we have $\delta \ll 1$ for $\theta \to 0, \pi$. A rough upper bound for the Bessel functions is for $\sigma \leqslant \delta$

$$|J_m(\sigma)| \leqslant (\tfrac{1}{2}\delta)^m/m!. \tag{4.2}$$

It follows that, for $\delta \ll 1$ and $m \neq 0$, the Bessel function J_m tends strongly to zero with increasing m, whereas only for $m = 0$, $J_0 \to 1$. As a consequence, we find from (3.10), (3.6) and (3.8) that, for $m \geqslant 1$ and $\theta \to 0°$ or 180°, $Z_m \to 0$; for $m = 0$ and $\theta \to 0°$,

$$Z_0 \to \frac{4\pi}{(1-UM)^3}\left\{\frac{\partial U}{\partial X} - i\pi StUM(2-UM)(1-UM)\right\}; \tag{4.3}$$

and, for $\theta \to 180°$,

$$Z_0 \to \frac{4\pi}{(1+UM)^3}\left\{\frac{\partial U}{\partial X} + i\pi StUM(2+UM)(1+UM)\right\}. \tag{4.4}$$

With respect to (3.12) this means that for $\theta \to 0, \pi$ the power spectral density of sound pressure W_{MT} consists only of the first member ($m = 0$) of the infinite series. The physical explanation of this phenomenon is that only axisymmetric components of turbulence can contribute to the sound radiation in the direction of

the jet axis. But one may ask whether there are axisymmetric components of turbulent pressure fluctuations in a circular jet at all, leading to non-negligible values of $\tilde{W}_{12,0}$. The experimental results in § 7 will indicate the presence of strong axisymmetric constituents for Strouhal numbers $0{\cdot}2 \leqslant St \leqslant 1$, whereas for $St > 2$ their strength is very small compared with that of the higher azimuthal constituents with $m \geqq 1$. It can be shown (cf. Michalke & Fuchs 1974) that, for the frequency range $0{\cdot}1 \leqq St \leqq 2$ important for jet noise (cf. Mollo-Christensen, Kolpin & Martuccelli 1964), both terms of (4.3) and (4.4) have to be taken into account.

For jet angles $0 < \theta < \pi$ the jet thickness parameter (4.1) increases as $\delta \sim StM \sin\theta$. As a consequence, additional contributions to the power spectral density W_{MT} of sound pressure will originate from the azimuthal constituents with $m \geqq 1$. Lighthill (1954) stated that, for a jet angle $\theta = 45°$, a maximum of sound radiation should occur for shear noise. Let us therefore discuss the term Z_m for $m = 0, 1, 2$, at a jet angle $\theta = 45°$, when, for simplicity, the small V component and dU/dX are neglected. From (3.10) and (3.6), we then find

$$\left.\begin{aligned} Z_0 &= -i\pi N^{-2}\left\{2N^{-1}\frac{\partial U}{\partial R}J_1(\sigma)+\sqrt{2}\,kD(1+N)\,UJ_0(\sigma)\right\},\\ Z_1 &= \pi N^{-2}\left\{N^{-1}\frac{\partial U}{\partial R}[J_0(\sigma)-J_2(\sigma)]-\sqrt{2}\,kD(1+N)\,UJ_1(\sigma)\right\},\\ Z_2 &= -i\pi N^{-2}\left\{N^{-1}\frac{\partial U}{\partial R}[J_1(\sigma)-J_3(\sigma)]-\sqrt{2}\,kD(1+N)\,UJ_2(\sigma)\right\}, \end{aligned}\right\} \tag{4.5}$$

where $$N = (1 - UM/\sqrt{2}) \quad \text{and} \quad \sigma = kDR/\sqrt{2}.$$

We see, from (4.5) and (3.12), that it is difficult to decide whether, at $\theta = 45°$, a maximum of sound radiation will occur or not, especially when the required double integration over the source volume and the unknown azimuthal constituents $\tilde{W}_{12,m}$ are considered. For small frequencies ($kD \ll 1$), however, we find, from (4.5), retaining only terms up to $O(kD)$,

$$\left.\begin{aligned} Z_0 &= -i\pi\sqrt{2}\,N^{-2}\left\{N^{-1}\frac{\partial U}{\partial R}\frac{R}{2}+(1+N)\,U\right\}kD,\\ Z_1 &= \pi N^{-3}\frac{\partial U}{\partial R},\\ Z_2 &= -i\pi N^{-3}\frac{\partial U}{\partial R}\,kD/2\sqrt{2}, \end{aligned}\right\} \tag{4.6}$$

and $Z_m = 0$ for $m \geqq 3$, to that order. It is obvious that in the limit $kD \to 0$ the term Z_1 dominates. From (3.12) it follows that, in that limit, a maximum of sound radiation can only occur if the first azimuthal constituent $\tilde{W}_{12,1}$ is different from zero. On the other hand, owing to (3.8), $kD \ll 1$ is equivalent to $StM \ll 0{\cdot}16$. This condition hardly holds for the Strouhal number range $0{\cdot}2 \leqq St \leqq 2$ important for jet noise.

At a right angle to the jet axis ($\theta = 90°$), Z_m is very small, since it is determined only by the small V component and its radial gradient. Therefore the sound

radiation normal to the jet axis caused by mean flow–turbulence interaction is, as known from previous results, very small.

Nevertheless, the importance of the contributions of the higher azimuthal constituents with $m \geqq 1$ can be estimated. Let us assume for a moment that the amount $|\tilde{W}_{12,m}|$ for all m is of the same order of magnitude. Then it follows from (3.10) that, for a fixed Strouhal number and Mach number (i.e. fixed kD), the magnitude of Z_m decreases with increasing m. This is obvious from the behaviour of the Bessel functions. For fixed argument σ, $J_m(\sigma)$ tends to zero for sufficiently large m (cf. Michalke & Fuchs 1974). For $M < 1$, we have, however, $\sigma \leqq \delta < 2\pi R^* St$, and can therefore estimate the number of azimuthal constituents which contribute most essentially to the power spectral density W_{MT} of the sound pressure for a given Strouhal number. It will become clear from the experimental results in § 7 that, at least for $0{\cdot}2 \leqq St \leqq 1$ and small Mach numbers, additionally the amount of $|\tilde{W}_{12,m}|$ decreases rapidly with increasing m.

Hence we can conclude that, for a fixed Mach number, the number of azimuthal constituents of turbulence contributing essentially to the sound power spectrum W_{MT} is most likely limited. This number depends on both the jet angle θ and the Strouhal number St. The largest number of constituents that have to be considered as important for jet noise will occur for $\theta = 90°$ and high Strouhal numbers. In order to estimate the magnitude of the various azimuthal constituents $|\tilde{W}_{12,m}|$, experiments have been carried out, which are described in the following.

5. Measuring procedure

A description of the jet rig used in the present investigation was given in Michalke & Fuchs (1974). Most of the measurements to be reported in this paper were done for an exit velocity $U_0 = 60\,\mathrm{m\,s^{-1}}$. At the corresponding Reynolds number $Re_D = 4 \times 10^5$ the nozzle boundary layer does not seem to be completely turbulent. In an investigation parallel to the present, this will be checked, and the effect of a trip wire on the downstream jet disturbances will be studied. The nozzle diameter was $D = 10\,\mathrm{cm}$. The possibilities of, and limitations on, direct fluctuating pressure measurements in turbulent flows were discussed in Fuchs (1970, 1972*b*). The proposed technique, which employs standard condenser microphones suitably fitted with a nose cone of streamlined shape, seems to be accepted by other experimenters, too, as may be inferred from Arndt & Nilsen (1966); Arndt, Tran & Barefoot (1972); Scharton & White (1972); Scharton, White & Rentz (1973); Nagamatsu & Sheer (1972); Nagamatsu, Sheer & Bigelow (1972); Meecham & Hurdle (1974). But Lau (1971) pointed out that, for higher Mach numbers above 0·7, this technique may become questionable, owing to several probing difficulties. A more sophisticated static pressure measuring device was described by Siddon (1969), who also gave some estimates of the probe-flow interference error.

In figure 1 logarithmic plots of spectra at $x = 3D$ for $U_0 = 60\,\mathrm{m\,s^{-1}}$ are depicted. The lower curve was taken with the $\frac{1}{4}$ in. microphone probe on the jet axis. Its linear fall-off between 360 Hz ($St = 0{\cdot}6$) and 1500 Hz ($St = 2{\cdot}5$) is followed by

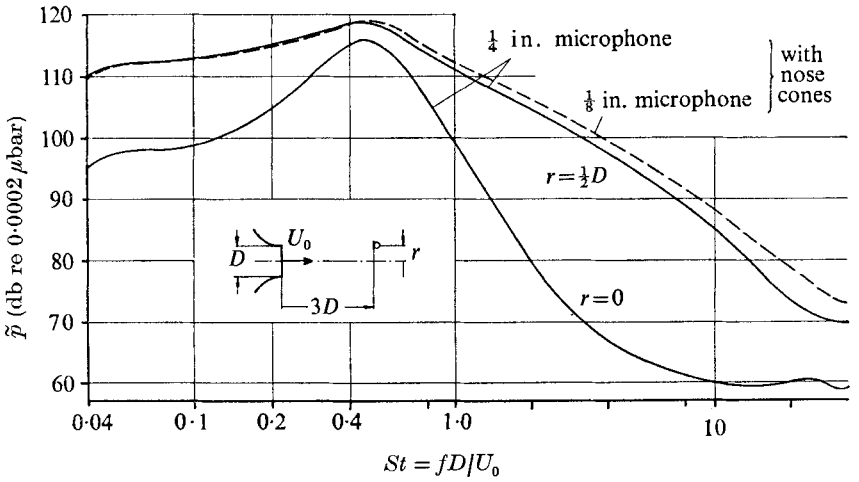

FIGURE 1. Pressure spectra $\tilde{p}(St)$ measured in a circular jet, in the plane $x = 3D$: averaging time 100 s; bandwidth $\Delta f = 10$ Hz; $U_0 = 60\,\mathrm{m\,s^{-1}}$.

a region where the dynamic range of the electronics (< 60 db) did not allow accurate measurements. Instead of the apparent levelling off at Strouhal numbers above 2·5, the true spectrum would more likely continue to fall.

The upper solid curve in figure 1 represents the spectrum measured at a position in the central mixing region. The dashed curve, as taken with the ⅛ in. pressure probe, indicates that, at higher frequencies corresponding to smaller turbulence scales, the resolution of the larger probe cannot be perfect. Furthermore, in this part of the turbulent flow there may still be other probe-flow interferences, too, which were discussed elsewhere. These, however, are not believed to invalidate the present experiments in the important range of Strouhal numbers between 0·1 and 1·8, where the pressure coherence measurements were performed. The signals detected by either the ¼ in. or ⅛ in. microphone probes were taken as at least a sufficiently close analogue to the true local pressure fluctuations in the flow with no probes inserted.

Figure 2 gives a survey of the r.m.s. pressure $\tilde{p}$ in both the potential core ($r = 0$) and mixing region ($r = \frac{1}{2}D$). The values for the two exit speeds 100 and 60 m s^{-1} are seen to collapse when $\tilde{p}$ is suitably normalized by $\rho_0 U_0^2$, as one would expect for an aerodynamic property of the undisturbed flow itself. It is worth noting that the overall pressure amplitude exhibits an absolute maximum at $x = 3D$, $r = \frac{1}{2}D$. Although the corresponding value at $r = 0$ is only one third of this maximum, figure 1 tells us that this is mainly due to the rapid decay of the lower and higher frequency components, whereas for Strouhal numbers around 0·45 the intensity varies only little across the jet (in fact less than 30 %).

The analog data analysis procedure is fairly standard and described elsewhere (cf. Michalke & Fuchs 1974). The coincident spectral density function (co-spectrum) of the pressure is defined as

$$C_\omega = \frac{1}{\Delta f T} \int_0^T p_1(f, \Delta f, t)\, p_2(f, \Delta f, t)\, dt \tag{5.1}$$

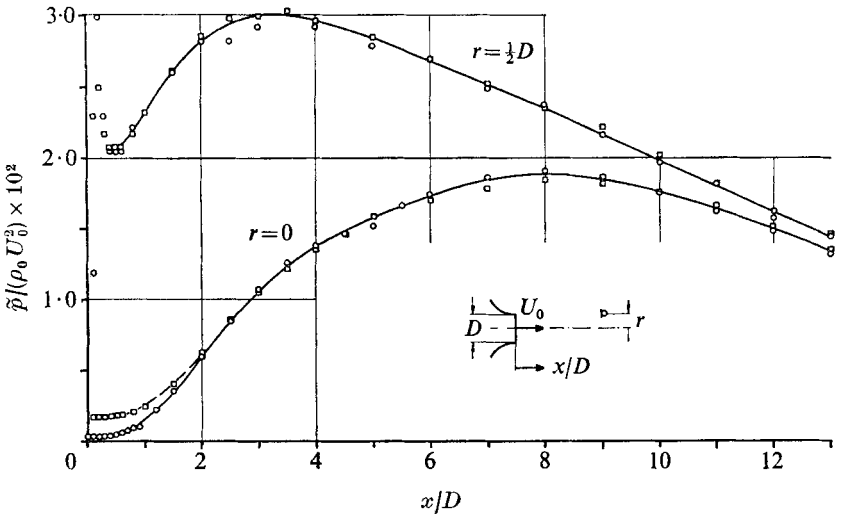

FIGURE 2. Variation of normalized pressure intensity along the jet in potential core and mixing region. U_0 (m s^{-1}): —○—, 60; —□—, 100.

for the limiting case $\Delta f \to 0$, $T \to \infty$. The corresponding quadrature spectral density function (quad-spectrum) is

$$Q_\omega = \frac{1}{\Delta f T}\int_0^T p_1(f, \Delta f, t)\, p_2^0(f, \Delta f, t)\, dt. \tag{5.2}$$

Both the functions C_ω and Q_ω are always normalized by the spectral densities,

$$\tilde{p}_\omega^2 = \frac{1}{\Delta f T}\int_0^T p^2(f, \Delta f, t)\, dt = \tilde{p}_\omega^{02}. \tag{5.3}$$

The p^0 signal is shifted 90° out of phase compared with the p signal at one of the filter outputs.

In order to keep the normalized random error small, i.e.

$$\epsilon \approx (\Delta f T)^{-\frac{1}{2}} \ll 1, \tag{5.4}$$

it is necessary to adjust the sampling or averaging time T according to the bandwidth Δf chosen in the filtering process. Most of the coherence measurements were done at filter mid-frequencies between 68 Hz and 1080 Hz corresponding to Strouhal numbers between 0·1125 and 1·8 (for $U_0 = 60$ m s^{-1}). A constant filter bandwidth Δf of 10 Hz was deemed sufficiently narrow to obtain optimized correlation results characteristic of the frequency components selected (i.e. to keep the frequency resolution error small). Preliminary tests then revealed that a sampling time T of approximately 200 s is necessary to produce practically the same results in repetitive samples, although $\epsilon \approx 2\,\%$ would seem too optimistic as a statistical error estimate in terms of a fractional portion of the measured correlation values.

6. Evaluation of space correlation data

6.1. *Cross-spectral density functions derived from two-point correlation measurements*

There has been some consideration of how to interpret narrow-band space correlations with respect to an appropriate model for the turbulence generating jet noise. When studying the statistical interdependence of signals detected at different axial positions, the downstream convection of the turbulence represents itself as a particularly strong coherence of certain narrow-band frequency components of the signals. The question whether such components should be attributed to 'wavelike' disturbances or 'frozen' turbulence was discussed in some detail by Fuchs (1972*b*). (See the appendix of that paper.)

In the context of the expansion scheme, which was developed in § 3, this question is irrelevant, since no restrictions were made concerning a specific structure of the turbulent field. The longitudinal correlation results cited above may be taken solely as a hint that the integration of (2.8) must be extended over much of the jet owing to $W_{p_1p_2}(\Delta x)$ being finite for axial displacements Δx of several jet diameters. This illustrates the importance of the interference function in the integral representation (2.8) of the far-field power spectrum W_{MT} owing to mean flow–turbulence interactions, which can be written in the compact form

$$W_{\mathrm{MT}} = F_0^2 \int_V dV_1 \int_V dV_2 W_{p_1p_2} H_{12}, \tag{6.1}$$

where $F_0 = \omega(4\pi\tilde{r}a_0^2)^{-1}$ and $H_{12} = \hat{L}_1 L_2 \exp[ik_i(y_{i2}-y_{i1})]$.

In this part of the paper, we take the decay function F_0 and interference function H_{12} as all being known or deducible from standard jet experiments or theory, and confine our attention to what cannot be assumed known from previous investigations: the cross-spectral density $W_{p_1p_2}$ of the fluctuating pressure in a turbulent jet.

It is not possible to determine the complex quantity $W_{p_1p_2}$ directly by analog techniques. But the cross-spectral density of the pressure fluctuations is easily derived from co- and quad-spectra estimates, according to (5.1) and (5.2). Departing from Bendat & Piersol's (1971) definition, in the relationship

$$W_{p_1p_2} = \tfrac{1}{2}(C_\omega + iQ_\omega), \tag{6.2}$$

the quadrature spectral density function Q_ω appears with positive sign.

6.2. *Symmetry considerations for a round jet*

Only for the special case of a more or less isotropic small-scale turbulence field would the functions involved in the integral solution (2.8) most suitably be described in Cartesian co-ordinates. If, however, one considers the sound radiation from large-scale coherent turbulence extending over the whole jet, co-ordinates should be chosen that are better adapted to the basically circular geometry of the jet and its source structure. The transformation from y_i to cylindrical co-ordinates, e.g.

$$W_{p_1p_2}(y_{i1}, y_{i2}) \rightarrow W_{p_1p_2}(X_1, R_1, \phi_1, X_2, R_2, \phi_2),$$

was made in § 3. Three types of symmetry assumptions may be valid in a round jet. Their fulfilment in the present model jet will simplify the experimental procedure in what follows.

(i) *Axisymmetric geometry.* With the geometry of the jet nozzle, plenum chamber, diffusor and muffler being strictly axisymmetric, one may define this axis of symmetry by optical means or by mean flow measurements. By preliminary plottings of velocity profiles normal to the jet it was possible to align the travelling probe supports such that $r = 0$ was well defined as a reference position for varying axial probe positions x.

(ii) *Circumferential homogeneity.* This condition requires that any time-averaged property of the flow should be independent of the angle ϕ. Likewise, there should not be a preferred azimuthal angle in the radiation characteristics, either. This homogeneity was checked experimentally within the flow; hence we have

$$W_{p_1 p_2} = W_{p_1 p_2}(X_1, R_1, X_2, R_2, \Delta\phi). \tag{6.3}$$

A real jet engine may fulfil this symmetry condition only in a limited sense. Any corrugations or notches at the nozzle, cellular structures or splitters near the efflux area would inevitably cause a dependence of data on the azimuth angle ϕ (or ϕ' in the far field).

(iii) *Circumferential isotropy.* Finally, a correlation function may, under certain circumstances, be independent of the sign of the angular displacement. Then we have

$$W_{p_1 p_2}(-\Delta\phi) = W_{p_1 p_2}(+\Delta\phi). \tag{6.4}$$

Such a symmetry condition would imply that, on a statistical average, disturbances should have no preference to travel in the positive or negative circumferential direction. This isotropy assumption was also checked in the model jet under investigation. But it may be less valid for a real jet when, for some reason, a mean swirl is superimposed on the exhaust flow before it leaves the nozzle exit.

6.3. *Azimuthal Fourier coefficients from circumferential correlations*

The basic idea in the expansion scheme of § 3 was to perform a Fourier decomposition of the jet noise source function (i.e. the CSD of the turbulent pressure). Equation (3.1) is rewritten here as

$$W_{p_1 p_2} = \sum_{m=-\infty}^{\infty} W_{12,m}(X_1, R_1, X_2, R_2) \exp(im\Delta\phi), \tag{6.5}$$

where homogeneity of the kind described in (6.3) was considered. If, finally, isotropy of the kind defined by (6.4) is taken into account, (6.5) may be written as

$$W_{p_1 p_2} = \sum_{m=0}^{\infty} \tilde{W}_{12,m}(X_1, R_1, X_2, R_2) \cos m\Delta\phi, \tag{6.6}$$

where the relation between $W_{12,m}$ and $\tilde{W}_{12,m}$ is defined by (3.13).

The corresponding azimuthal constituents of the far-field sound pressure PSD can be written in a more compact form of (3.12) as

$$W_{\mathrm{MT},m} = F^2 \int_V dV_{a1} \int_V dV_{a2} \tilde{W}_{12,m} F_{r,m} F_x, \tag{6.7}$$

where the decay function

$$F = M^2 St(4\pi \tilde{R} U_0 D)^{-1},$$

the radial interference function

$$F_{r,m} = \hat{Z}_{m,1} Z_{m,2} U_0^2/D^2,$$

the axial interference function

$$F_x = \exp[-ikD\cos\theta(X_2 - X_1)],$$

and the annular volume element

$$dV_a = D^3 2\pi R\, dR\, dX.$$

The azimuthal constituents $\tilde{W}_{12,m}$ contained in (6.7) are simply related to the measured co- and quad-spectra. Comparing (6.6) and (6.2), we find

$$\tilde{W}_{12,m} = \tfrac{1}{2}(C_{\omega,m} + iQ_{\omega,m}). \tag{6.8}$$

The real Fourier coefficients $C_{\omega,m}$ and $Q_{\omega,m}$ are the computational result of a Fourier analysis of the measured functions $C_\omega(\Delta\phi)$ and $Q_\omega(\Delta\phi)$ with the frequency f or Strouhal number St held constant in each set of narrow-band correlations:

$$C_\omega(\Delta\phi) = \sum_{m=0}^{\infty} C_{\omega,m}\cos m\Delta\phi, \quad Q_\omega(\Delta\phi) = \sum_{m=0}^{\infty} Q_{\omega,m}\cos m\Delta\phi, \tag{6.9}$$

at constant axial and radial position (X_1, R_1) and (X_2, R_2).

To illustrate the general computational procedure, the special case of purely circumferential correlations with

$$X_1 = X_2 = X \quad \text{and} \quad R_1 = R_2 = R$$

is considered here (i.e. these measurements are done in a plane normal to the jet axis). In this special case, Q_ω is found to be identically zero within the measuring accuracy. This is a logical consequence of the isotropy condition; for a finite Q_ω would imply that a definite phase difference $\gamma(\Delta\phi, f)$ exists (on a statistical average), the magnitude of which results from

$$\tan\gamma = Q_\omega/C_\omega. \tag{6.10}$$

But this would indicate a definite tendency of the jet disturbances to travel (or be convected) in one particular circumferential direction. That seems not impossible; but it would be incompatible with the isotropy assumption for a strictly axisymmetric circular jet (compare § 6.2).

Another characteristic feature of the purely circumferential correlation is that the Fourier coefficients are equivalent to the PSD of the individual azimuthal constituents of the fluctuating pressure. This follows from (6.9) for $\Delta\phi = 0$:

$$\text{PSD} = C_\omega(0) = \sum_{m=0}^{\infty} C_{\omega,m}(X,R) = \sum_{m=0}^{\infty} \tilde{p}^2_{\omega,m}(X,R). \tag{6.11}$$

On the other hand, (5.1) (and similarly (5.3)), in this special case, can be written as

$$C_\omega(0) = \tilde{p}^2_\omega = \tilde{p}^2(f,\Delta f)/\Delta f \quad \text{for} \quad \Delta f \to 0. \tag{6.12}$$

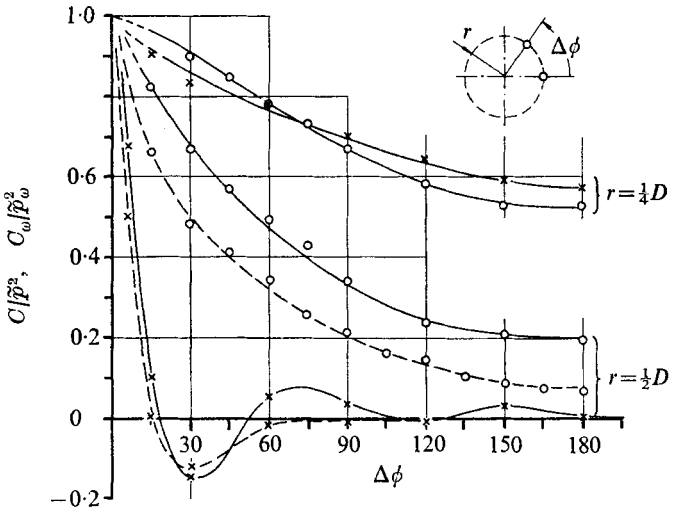

FIGURE 3. Azimuthal correlation coefficients in the plane $x = 3D$, at constant radii, for $St = 0{\cdot}45$, $\Delta f = 10\,\mathrm{Hz}$, $U_0 = 60\,\mathrm{m\,s^{-1}}$: – – –, broad-band; ——, narrow-band analysis; ×, velocity correlation; ○, pressure correlation.

An appropriate way of normalizing the coefficients is therefore a division by $\tilde{p}^2_\omega$:

$$\frac{C_\omega(0)}{\tilde{p}^2_\omega} \equiv 1 = \sum_{m=0}^{\infty} \frac{C_{\omega,m}(X,R)}{\tilde{p}^2_\omega(X,R)}. \tag{6.13}$$

$C_{\omega,m}/\tilde{p}^2_\omega$ then describes the percentage of fluctuating energy contained in the mth azimuthal constituent of the fluctuating quantity for the particular values of the parameters X, R and f (or St).

In practice, a finite number has to be chosen for m to approximate the measured $C_\omega(\Delta\phi)/\tilde{p}^2_\omega$ by azimuthal constituents $C_{\omega,m}/\tilde{p}^2_\omega$. $m = 16$ was deemed sufficient here, since most of the energy of the fluctuating pressure field was found in the lower-order azimuthal constituents anyway. This is quite obvious from the circumferential correlation curves at $x = 3D$, which were plotted as a typical example in figure 3. The two upper solid curves represent measurements with pressure and hot-wire probes positioned at $r = \frac{1}{4}D$ in the jet core region with the filter frequency set at a Strouhal number $St = 0{\cdot}45$. The intimate connexion between p' and the longitudinal velocity fluctuations u' in this flow region was discussed by Fuchs (1972*a*); it is here seen to result in almost identical coherence curves.

In the jet mixing region ($r = \frac{1}{2}D$), however, the statistical character of both signals differs considerably. This difference is brought out most strikingly by the two lower solid curves, which were measured at the same location in the jet, and again at a Strouhal number of 0·45. They were therefore chosen to illustrate the method of azimuthal Fourier decomposition of fluctuating field quantities. The Fourier analysis of a large number of circumferential correlations is done on a digital computer. $m = 16$ values for $C_\omega/\tilde{p}^2_\omega$ are taken at equidistant angular displacements $\Delta\phi$ from interpolated correlation curves, like those depicted in figure 3, which ought to be symmetrically completed for $180° \leqslant \Delta\phi \leqslant 360°$.

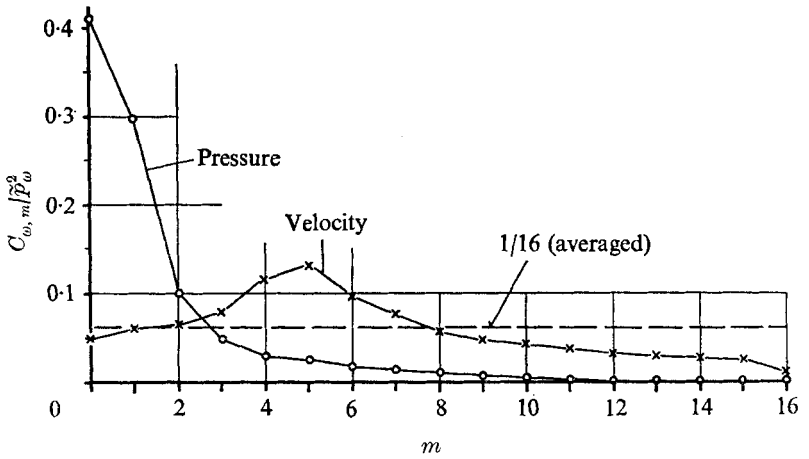

FIGURE 4. Resolution of turbulent pressure and velocity correlations into $m = 16$ azimuthal coefficients, from data in figure 3, for $r = \frac{1}{2}D$, $St = 0{\cdot}45$.

The result of the analysis for the pressure at $r = \frac{1}{2}D$ in figure 4 shows that the lower-order azimuthal constituents $m = 0, 1, 2, 3$ are by far the strongest for this particular frequency component. With the dashed horizontal line in figure 4 indicating the fictitious case when the fluctuating energy is evenly distributed over all azimuthal constituents, one may conclude that constituents with $m > 3$ are clearly under-represented. In fact, they are almost negligible for $m \geqslant 10$, thus justifying a restriction to only $m = 16$ constituents in this approximate Fourier analysis.

In figure 4 there are also shown the corresponding azimuthal coefficients of the axial velocity fluctuations in exactly the same flow region where the pressure was measured. A more even distribution is apparent, although in this case azimuthal constituents for m around 5 seem still to dominate by a factor of 2 in relation to the average.

The marked difference between the pressure and axial velocity in the mixing region manifests itself, once again, in the amount of energy contained in the axisymmetric (ring-vortex) constituents ($m = 0$) of both fluctuating quantities (42 % of the m.s. pressure compared with only 5 % of the m.s. velocity). This difference would be even more pronounced (namely, 29–1·3 %) had the corresponding broad-band correlations (dashed curves in figure 3) been analysed. This may help to explain why large-scale coherent turbulence structures were often overlooked in correlation analyses with hot-wire probes in the mixing region of a jet.

7. Resolution of turbulent pressure field into azimuthal constituents

7.1. *Power spectral density of lower-order azimuthal constituents*

Narrow-band circumferential correlations of the kind described in § 6.3 were performed in planes normal to the jet axis at $x/D = 1$, 3, 6 and 12. These complement earlier pressure correlation measurements reported by Fuchs (1972*b*)

which dealt mainly with longitudinal Δx and lateral Δr probe displacements and with a separation of the axisymmetric $m = 0$ constituent from the rest of the turbulence. The circumferential separation of the probes $\Delta\phi$ was made in steps of 15–30°, depending on the gradient of the correlation curve. The measurements were done at $St = 0{\cdot}1125$, $0{\cdot}225$, $0{\cdot}45$, $0{\cdot}9$, $1{\cdot}8$, and for constant radii $r/D = \frac{1}{4}$, $\frac{1}{2}$ and $\frac{2}{3}$, 1, $\frac{3}{2}$. All except the one at $x = D$, $r = \frac{1}{4}D$ were made in the turbulent mixing zone of the jet.

The resulting correlations are not reproduced here. Instead, the normalized Fourier coefficients $C_{\omega,m}/\tilde{p}_\omega^2$ were plotted in figure 5 for m from 0 to 5, and only one measuring plane $x = 3D$, selected for illustration. (For more comprehensive experimental results the reader may refer to Michalke & Fuchs 1974.) The percentage of energy contained in the azimuthal constituents with $m \geqslant 5$ is almost negligible within the range of Strouhal numbers selected, the corresponding computational results being omitted here, and in the evaluations to follow.

The results depicted in figure 5 show a pronounced peak of the $m = 0$ constituent at $St = 0{\cdot}45$ for all radial positions. In contrast, for frequencies both sides of this peak, the $m = 1$ constituent seems to dominate across the jet. The relative strength of the rest of the constituents shows only little variation with r. There is a clear tendency of these higher azimuthal constituents ($1 \leqslant m \leqslant 5$) to become more prominent for higher St. The same trend is also visible for St well below $0{\cdot}45$. A comparison of the experimental data obtained at different axial positions shows only a slight change in the results for $r = \frac{1}{4}D$, but some marked variations in the $r = \frac{1}{2}D$ data. Closer to the nozzle edge, the $m = 1$ constituents obviously dominate for all frequencies, whereas the $m = 0$ and $m = 2$ fluctuations of the pressure are approximately equal in strength. The results further downstream ($x = 6$ and $12D$) indicate that there the axisymmetric constituents become less prevailing too, except for the small value of r. Right on the axis ($r = 0$) only the axisymmetric pressure component can exist owing to symmetry considerations.

The measurements at four discrete St were interpolated linearly in figure 5. The values at intermediate Strouhal numbers were also used in the following evaluation for the spectra of the first four or five azimuthal constituents of the pressure in the plane $x = 3D$ as shown in figures 6 (*a*)–(*c*). The equations (6.11)–(6.13) were used to obtain the respective non-dimensional normalized PSD of the mth constituent:

$$\frac{\tilde{p}_m^2(f)/(\rho_0 U_0^2)^2}{\Delta f D/U_0} = \frac{C_{\omega,m}}{\tilde{p}_\omega^2} \frac{\tilde{p}^2(f)/(\rho_0 U_0^2)^2}{\Delta f D/U_0}. \tag{7.1}$$

$\tilde{p}^2(f)$ is the directly measured (non-resolved) m.s. pressure filtered at a frequency f and bandwidth Δf. The normalized form of $\tilde{p}^2(f)$, which appears in (7.1) as a multiplier for the normalized Fourier coefficients, was plotted in figures 6 (*a*)–(*c*), along with the PSD's of the individual azimuthal pressure constituents.

Different vertical scaling was used in figures 6 (*a*)–(*c*). The non-resolved PSD attains a maximum in the middle of the mixing region (figure 6 (*b*)) and decays very rapidly towards the entrainment region (figure 6 (*c*)). With increasing r the spectral peak is slightly shifted towards lower St. The PSD of the axisymmetric

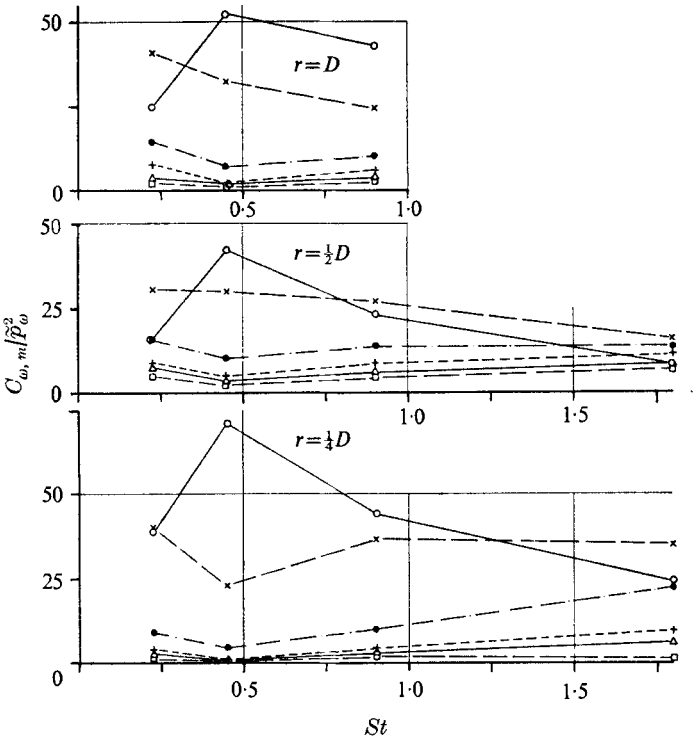

FIGURE 5. Percentage of energy contained in low-order azimuthal constituents of fluctuating pressure field. Correlation and Fourier analysis at $x = 3D$, $U_0 = 60\,\mathrm{m\,s^{-1}}$. m: ○—○, 0; ×—×, 1; ○—·—·—○, 2; +---+, 3; △—△, 4; □---□, 5.

constituent ($m = 0$) shows but little change for $r = \frac{1}{4}D$ and $r = \frac{1}{2}D$ whereas the $m = 1, 2, 3, 4$ constituents have strengthened by a factor between 2 and 4. In the important range of St between 0·1 and 1·0 the decay for $r > \frac{1}{2}D$ is strongest for the axisymmetric pressure disturbance, the shift of the peak frequency being most pronounced for the higher azimuthal constituents.

7.2. *Variation along the jet of azimuthal frequency components*

In this subsection the results of the Fourier analysis of circumferential correlations (at $r = \frac{1}{2}D$) are considered as a function of downstream location. The normalized Fourier coefficients were plotted against x/D in figure 7, with the four Strouhal numbers selected as a parameter ($St = 0{\cdot}225$, 0·45, 0·9 and 1·8). These four diagrams reveal a very important result: the azimuthal constituent with $m = 1$ clearly dominates along $r = \frac{1}{2}D$ over the whole of the noise-producing jet region, and not the axisymmetric component. Differing statements in earlier publications, which overestimated the importance of the axisymmetric content in the pressure field at $r = \frac{1}{2}D$, may readily be explained by figure 7. Most of the earlier space correlations were done at $St = 0{\cdot}5$ or 0·45, and around $x = 3D$. Actually, only in this rather limited range of parameters does the $m = 0$ constituent dominate, as may be seen from figure 7 (*b*).

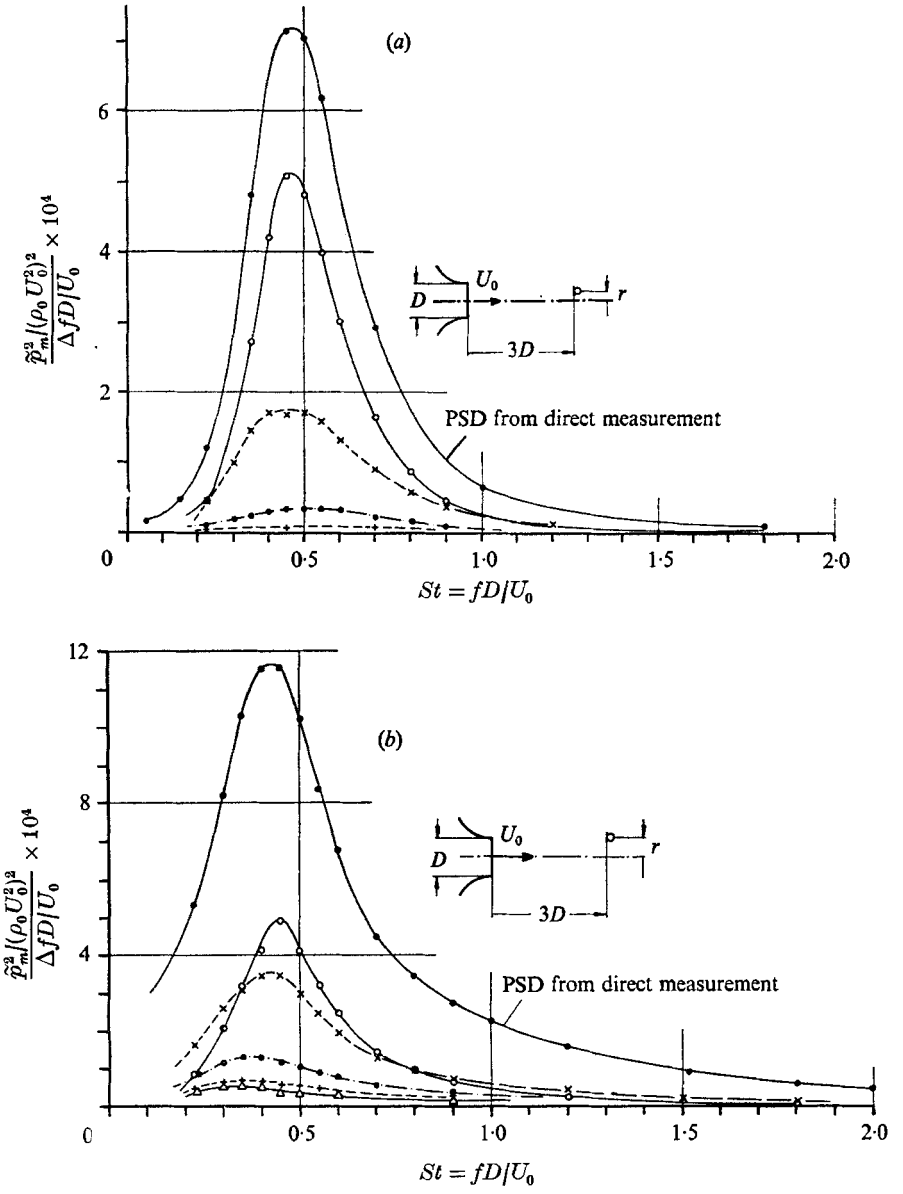

FIGURES 6(*a*, *b*). For legend see next page.

The following was not so clear from the previous plottings: consideration of the sequence figures 7 (*a*)–(*d*) (St = 0·225, 0·45, 0·9, 1·8, respectively) most vividly shows that the different St-components attain their maximum intensity level at widely separated axial positions in the mixing region, no matter which azimuthal constituent is considered. The vertical scaling was not varied in figure 7, in order to visualize the relative magnitudes of the different frequency components. The St = 0·45 component undoubtedly shows the biggest variations in the downstream direction and the strongest energy concentration at $x = 3D$.

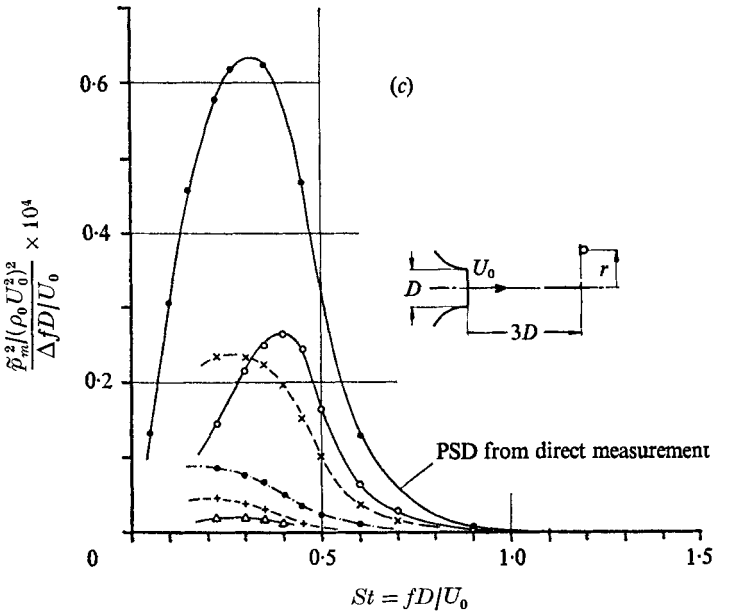

FIGURE 6. Normalized PSD of azimuthal constituents of jet pressure, from (7.1) and data in figure 5, for $x = 3D$. Symbol key as for figure 5. r: (*a*) $\frac{1}{4}D$; (*b*) $\frac{1}{2}D$; (*c*) D.

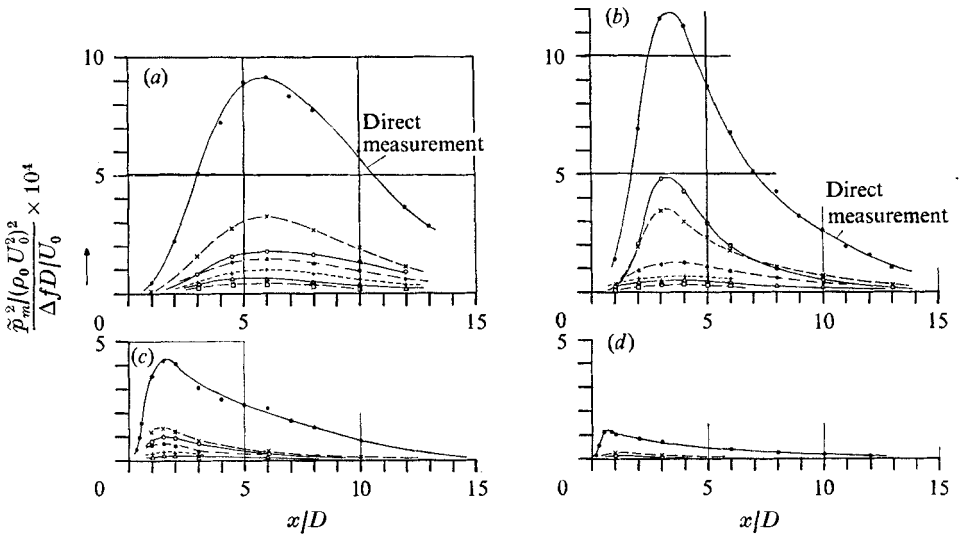

FIGURE 7. Variation along the jet of azimuthal frequency components of the pressure, for $r = \frac{1}{2}D$. Symbol key as for figure 5. St: (*a*) 0·225; (*b*) 0·45; (*c*) 0·9; (*d*) 1·8.

Unfortunately, no circumferential correlations were performed at $St < 0{\cdot}225$. Therefore, only the non-resolved frequency component at $St = 0{\cdot}1125$ was plotted, along with the corresponding r.m.s. pressure of the other frequency components in figure 8. $\tilde{p}(f)$ as a function of x/D was normalized by twice the stagnation pressure at the jet exit plane. The trend of such intensity plots to peak

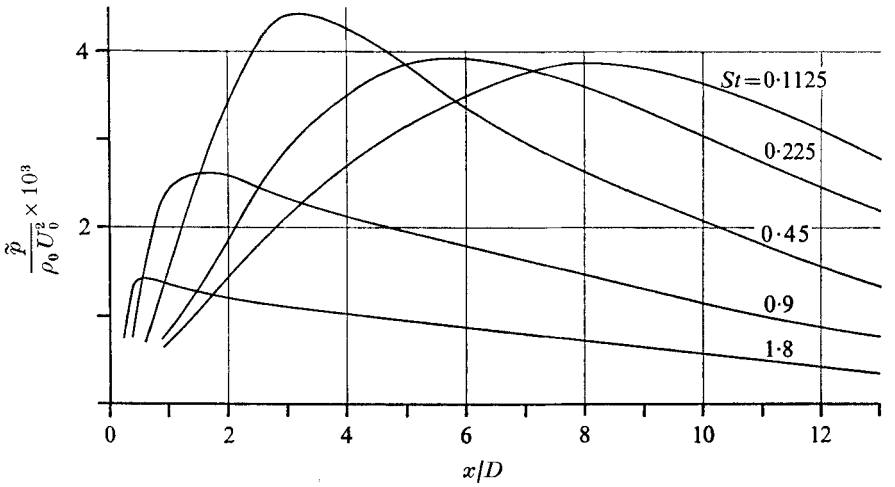

FIGURE 8. Variation along the jet of unresolved frequency components of the pressure, for $r = \frac{1}{2}D$.

further downstream the lower the Strouhal number is seen to continue with the $St = 0{\cdot}1125$ component, which reaches a maximum as far as 8 diameters downstream.

From figures 7 and 8, one may deduce that halving of the frequency is coupled with, roughly, doubling the distance from the jet exit where the individual frequency components reach their maximum level. The lower the maximum level is, the slower does the intensity decay downstream of it. The ascent towards the maximum, on the other hand, becomes monotonically steeper for increasing St.

The association of different downstream flow regions with characteristic frequencies or scales of the turbulent motion reflects the development of the turbulent structure as it convects and reorganizes in a shear layer of steadily broadening width. This cascade-like appearance of bigger vortices following the smaller ones is in agreement with existing models of the large-scale coherent structures as will be discussed later. Apart from this, figure 8 may serve as a valuable supplement to the overall pressure intensity survey in figure 2.

8. Discussion of experimental results

A new experimental method has been constructed, which enables one to make a straightforward quantitative analysis of the fluctuating pressure field in a circular air jet. It is based on narrow-band circumferential space correlations. It is particularly appropriate for studying large-scale coherent phenomena in jet turbulence which, so far, have mainly been described by means of more qualitative flow visualization techniques. The fluctuating energy contained in a narrow frequency band is split into azimuthal constituents and then plotted as a suitably normalized PSD for a given axial and radial location in the jet.

Figures 6 (*a*)–(*c*) show the variation of the spectra in a plane normal to the jet, which was chosen to lie at $x = 3D$, where, according to figure 2, the overall fluctua-

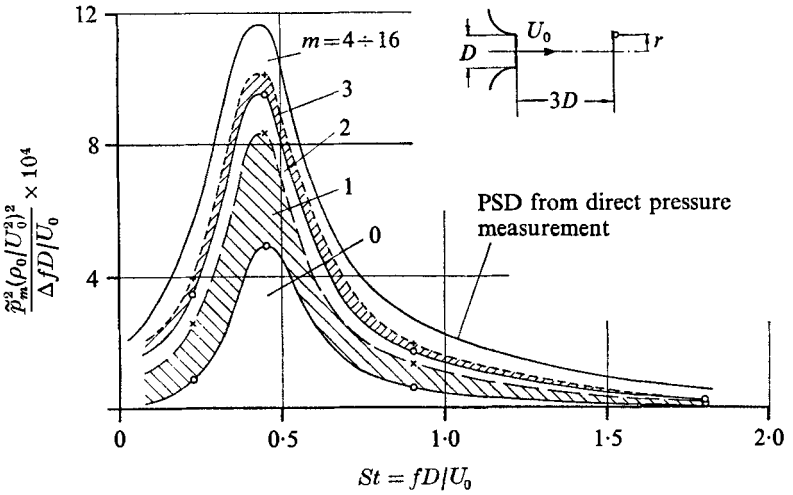

FIGURE 9. Synthesis of normalized PSD of jet pressure from $m = 16$ azimuthal constituents for $x = 3D$, $r = \frac{1}{2}D$.

tions are obviously strongest. The dominance of the axisymmetric constituent of the pressure is most obvious in the potential core region (figure 6 (*a*)). By far most of the energy is contained in the range of Strouhal numbers between 0·1 and 1. The variation of individual azimuthal frequency components along a path $r = \frac{1}{2}D$ parallel to the jet axis (figures 7 (*a*)–(*c*)) clearly demonstrates that, for x/D between 1 and 10, it is justifiable to approximate the pressure by its four lowest azimuthal constituents.

A superposition of the $m = 0, 1, 2, 3$ constituents in figure 9 (reproduced from Fuchs 1974) in fact visualizes this rather unexpected situation; and it is an essential result to be reported in this paper. It is entirely independent of the theoretical analysis for the radiation field, which was not meant to predict the composition of the source quantity. Nevertheless, it has an enormous impact on the particular jet noise expansion scheme put forward in this paper. Since the latter predicts an excellent efficiency for these lower-order pressure constituents in generating noise, both results complement each other in a most profitable way. They help reduce the vast amount of correlation data required to evaluate an integral solution of the form (6.7).

It is pointed out here that we restricted our attention to a limited range of St, since we were primarily interested in that part of the turbulent pressure which most likely determines the jet noise emission. A more comprehensive study of the whole turbulence spectrum would probably reveal, for Strouhal numbers below 0·2 and above 1, a more even distribution of energy over the m azimuthal constituents. Such a tendency is obvious from figure 5. Likewise, we were primarily interested in that part of the jet between $x/D = 1$ and 12, which is known to be mainly responsible for the jet noise emission. It may be surmised, from figure 7, that, in the transition region further downstream, the balance between the azimuthal constituents may again differ considerably from that in the core and mixing regions.

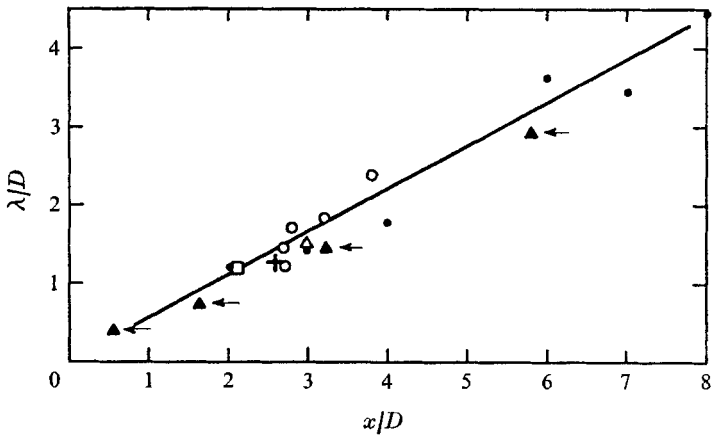

FIGURE 10. Mean separation distance between neighbouring large-scale structures in a jet, after Laufer *et al.* (1974). Arrows indicate results from evaluation of extrema in figure 8, using (8.2) with $U_c/U_0 = 0{\cdot}65$. ●, Peterson; □, Ko & Davies; △, Fuchs; +, Lau, Fisher & Fuchs; ○, Crow & Champagne.

The association of different downstream flow regimes with varying longitudinal and lateral scales of the turbulence pattern deducible from figure 8 leads to an important extension of the Lau *et al.* (1972) model of evenly spaced ring vortices. In a more realistic view of the continuous flow development in the mixing region, one may assume that the scale of the coherent structures λ is roughly proportional to the local width L_r of the shear layer, which itself increases linearly with distance x from the nozzle:

$$\lambda \sim L_r \sim x. \tag{8.1}$$

This fact was first emphasized by Laufer, Kaplan & Chu (1974). Their corresponding figure 3 is reproduced here as figure 10 with the experimental data evaluated from the occurrence of the peaks in figure 8 added as dark triangles. A constant convection velocity U_c of $0{\cdot}65U_0$ was taken to relate frequencies and scales of the structures:

$$\frac{\lambda}{D} = \frac{U_c}{fD} = \frac{U_c/U_0}{St}. \tag{8.2}$$

Useful comparative material for the proportionality assumption $St \sim x^{-1}$ may also be found in Arndt *et al.* (1972, figure 24) and from the results of Chan (1974*a*).

With respect to the pairing process of neighbouring vortices, which Laufer *et al.* (1974) believe to be the key to the understanding of the turbulent mixing process and to the noise generation as well, it is noted that any kind of purely axisymmetric ring vortex model does not take into account the next higher azimuthal components, which, as was shown in § 7, may be of the same order of magnitude in fluctuating energy. As far as the pressure field in the mixing zone is concerned (figure 7), it is the $m = 1$ constituent that clearly dominates. This component may be thought of as being associated with a random, fish-tail, wiggling type of motion in the jet. In other words, having replaced the picture of entirely disordered fine-scale turbulence by a model of relatively ordered large-scale coherent structures, one is now urged not to oversimplify the actual situation in

a turbulent jet by confining oneself exclusively to the $m = 0$ components, which always remain phase-locked circumferentially.

The behaviour of the jet pressure fluctuations as they propagate down the jet was discussed by Fuchs (1972*b*), on the basis of narrow-band longitudinal correlation measurements. The wavelike character observed is not considered here; for it has no direct impact on the expansion scheme put forward in this paper. The latter would be applicable even if the coherence in the streamwise direction were less pronounced. It may be recalled, however, that high coherence of turbulent fluctuations at widely displaced locations in a jet was first discovered for longitudinal and lateral displacements of the measuring probes.

9. Conclusions

The investigations reported are part of a continuing effort to analyse fully the statistical properties of the fluctuating pressure field in turbulent model jets with respect to the jet noise problem. The analysing technique employed has proved useful, because it enables measurement of exactly those quantities involved in an integral representation for the far-field sound pressure PSD like that in (6.7).

The experimental results so far have shown, in definite figures, exactly how strong the more coherent part of the pressure field is in a selected plane $x = 3D$ normal to the jet axis. Still a lot remains to be done in cross-correlation or cross-spectral density measurements including all three: longitudinal, lateral and azimuthal probe separations. It is hoped that studies along these lines will finally enable the introduction of a realistic turbulence model into the jet noise theory as based on Lighthill and further developed by Michalke to take into account certain aspects of axisymmetric shear flows in particular.

A conclusion which can be drawn from the present experimental and theoretical results (as far as the jet noise produced by mean flow–turbulence interaction is concerned) is that most of the radiated noise in the important Strouhal number range $0{\cdot}2 \leqslant St \leqslant 1$ can be associated with only a small number of low-order azimuthal components of the jet turbulence.

The intimate connexion between the large-scale coherent jet structures and instability mechanisms in the turbulent (finite-thickness) shear profile was often conjectured, e.g. by Ffowcs Williams (1974) in his evaluation report of the 1973 AGARD Specialists' Meeting on Noise Mechanisms, and by Chan (1974*a*). Several researchers have worked on instability theories that take into account the steadily growing shear-layer width, and the effect of solid boundaries at the origin of the flow.

Another possible sideway, which would by-pass some of the tremendously time-consuming correlation measurements, could be to introduce into the theory of suitable models for the longitudinal (nearly wavelike) and lateral correlations on the basis of already available experimental evidence and investigate the effect of moderate deviations from these model assumptions on the radiation pattern. A first step in this direction may be seen in a short note by Chan (1974*b*).

Finally, an attempt will be made to modify the turbulence structure in such a way that it becomes less coherent, and thereby less efficient in generating sound. The quin-axial jet noise suppressor of Scharton & White (1972), and the characteristics of the screen-perturbed jets of Arndt *et al.* (1972) are taken as promising hints that there may still be space for novel developments in the thicket of jet noise research and abatement.

Some of the correlation measurements were performed by F. Bischoping and described in his diploma thesis. R. R. Armstrong, who recently joined the group, provided valuable data confirming the validity of the pressure measuring devices. The authors wish to thank members of the two institutes who, in so many ways, enabled the preparation of this paper. Thanks are also due to the Deutsche Forschungsgemeinschaft, who kindly provided financial support during the course of the work.

Appendix

The inviscid momentum equation is in the source region

$$\rho\frac{\partial c_i}{\partial t}+\rho c_k\frac{\partial c_i}{\partial y_k}+\frac{\partial p}{\partial y_i}=0. \tag{A 1}$$

Scalar multiplication by the unit vector $x_i/\tilde{r}$ yields the component of the vector equation (A 1) in the x_i direction, as indicated by the index r:

$$\rho\frac{\partial c_r}{\partial t}+\rho c_k\frac{\partial c_r}{\partial y_k}+\frac{\partial p}{\partial y_r}=0. \tag{A 2}$$

Multiplication of (A 2) by nc_r^{n-1} leads to

$$\rho\frac{\partial}{\partial t}(c_r^n)+\rho c_k\frac{\partial}{\partial y_k}(c_r^n)+nc_r^{n-1}\frac{\partial p}{\partial y_r}=0. \tag{A 3}$$

Adding the continuity equation multiplied by c_r^n to (A 3), the latter can be written as

$$\frac{\partial}{\partial t}(\rho c_r^n)+\frac{\partial}{\partial y_k}(\rho c_k c_r^n)+nc_r^{n-1}\frac{\partial p}{\partial y_r}=0. \tag{A 4}$$

If we take the time derivative of (A 4), evaluate it at the retarded time and integrate the equation over the source region V, then the following equation is obtained:

$$\int_V dV\left[\frac{\partial^2}{\partial t^2}(\rho c_r^n)\right]=n\int_V dV\left[\frac{\partial}{\partial t}\left(p\frac{\partial c_r^{n-1}}{\partial y_r}\right)+\frac{1}{a_0}\frac{\partial^2}{\partial t^2}(pc_r^{n-1})\right]+\frac{1}{a_0}\int_V dV\left[\frac{\partial^2}{\partial t^2}(\rho c_r^{n+1})\right], \tag{A 5}$$

where use has been made of the far-field approximation valid for any function f vanishing at the surface of V:

$$\int_V dV\left[\frac{\partial f}{\partial y_k}\right]\approx-\frac{1}{a_0}\frac{x_k}{\tilde{r}}\int_V dV\left[\frac{\partial f}{\partial t}\right]. \tag{A 6}$$

For $n = 2$, the left-hand side of (A 5) is identical with the integral of the Lighthill solution (2.4). Therefore it can be replaced by the right-hand side of (A 5), yielding

$$p_S = \frac{1}{4\pi\tilde{r}}\frac{1}{a_0^2}\left\{\int_V dV\left[2\frac{\partial}{\partial t}\left(p\frac{\partial c_r}{\partial y_r}\right)+\frac{2}{a_0}\frac{\partial^2}{\partial t^2}(pc_r)\right]+\frac{1}{a_0}\int_V dV\left[\frac{\partial^2}{\partial t^2}(\rho c_r^3)\right]\right\}. \quad \text{(A 7)}$$

The last term of (A 7) can again be replaced by means of (A 5) for $n = 3$. Then, after repeated applications of (A 5), (A 7) leads to

$$p_S(x_i,t) = \frac{1}{4\pi\tilde{r}}\frac{1}{a_0^2}\int_V dV\left[\frac{\partial}{\partial t}\left\{p\frac{\partial}{\partial y_r}(2c_r+3c_rM_r+4c_rM_r^2+5c_rM_r^3+\ldots)\right\}\right.$$
$$\left.+\frac{1}{a_0}\frac{\partial^2}{\partial t^2}\{p(2c_r+3c_rM_r+4c_rM_r^2+5c_rM_r^3+\ldots)\}\right], \quad \text{(A 8)}$$

where $M_r = c_r/a_0$. For $M_r < 1$ the term in the brackets ( ) can be written as

$$(\ ) = \frac{2-M_r}{(1-M_r)^2}c_r, \quad \frac{\partial}{\partial y_r}(\ ) = \frac{2}{(1-M_r)^3}\frac{\partial c_r}{\partial y_r}. \quad \text{(A 9)}$$

Therefore the alternative form of the Lighthill integral solution (2.4) is, for $M_r < 1$,

$$p_S(x_i,t) = \frac{1}{4\pi\tilde{r}}\frac{1}{a_0^2}\int_V dV\left[\frac{\partial}{\partial t}\left\{\frac{2p}{(1-M_r)^3}\frac{\partial c_r}{\partial y_r}\right\}+\frac{1}{a_0}\frac{\partial^2}{\partial t^2}\left\{\frac{pc_r(2-M_r)}{(1-M_r)^2}\right\}\right]. \quad \text{(A 10)}$$

It should be emphasized that the powers of $(1-M_r)$ appearing in (A 10) are a consequence of the series (A 8). They are completely different from convective amplification terms of the type $(1-M_c\cos\theta)^{-n}$, which have been derived by e.g. Jones (1968), when the turbulence is considered in a frame of reference moving with the convection speed U_c of eddies.

REFERENCES

Arndt, R. E. A. & Nilsen, A. W. 1966 On the measurement of fluctuating pressure in the mixing zone of a round jet. *A.S.M.E. Publ.* no. 71-FE-31.

Arndt, R. E. A., Tran, N. & Barefoot, G. 1972 Turbulence and acoustic characteristics of screen perturbed jets. *A.I.A.A. Paper*, no. 72-644.

Bendat, J. S. & Piersol, A. G. 1971 *Random Data: Analysis and Measurement Procedures*. Wiley.

Chan, Y. Y. 1974*a* Spatial waves in turbulent jets. *Phys. Fluids*, **17**, 46–53.

Chan, Y. Y. 1974*b* Pressure sources for a wave model of jet noise. *A.I.A.A.J.* **12**, 241–242.

Crow, S. C. & Champagne, F. H. 1971 Orderly structure in jet turbulence. *J. Fluid Mech.* **48**, 547–591.

Ffowcs Williams, J. E. 1974 Noise mechanisms. *AGARD-CP*-131, *Tech. Eval. Rep.* A 1–16.

Fuchs, H. V. 1970 Über die Messung von Druckschwankungen mit umströmten Mikrofonen im Freistrahl. *DLR-FB*, no. 70-22.

Fuchs, H. V. 1972*a* Measurement of pressure fluctuations within subsonic turbulent jets. *J. Sound Vib.* **22**, 361–378.

Fuchs, H. V. 1972*b* Space correlations of the fluctuating pressure in subsonic turbulent jets. *J. Sound Vib.* **23**, 77–99.

Fuchs, H. V. 1974 Resolution of turbulent jet pressure into azimuthal components. *AGARD-CP*-131, paper 27.

JONES, I. S. F. 1968 Aerodynamic noise dependent on mean shear. *J. Fluid Mech.* **33**, 65–72.

LAU, J. C. 1971 The coherent structure of jets. Ph.D. thesis, University of Southampton.

LAU, J. C., FISHER, M. J. & FUCHS, H. V. 1972 The intrinsic structure of turbulent jets. *J. Sound Vib.* **22**, 379–406.

LAUFER, J., KAPLAN, R. E. & CHU, W. T. 1974 On the generation of jet noise. *AGARD-CP*-131, paper 21.

LIGHTHILL, M. J. 1952 On sound generated aerodynamically. I. General theory. *Proc. Roy. Soc.* A **211**, 564–587.

LIGHTHILL, M. J. 1954 On sound generated aerodynamically. II. Turbulence as a source of sound. *Proc. Roy. Soc.* A **222**, 1–32.

LILLEY, G. M. 1958 On the noise from air jets. *Aero. Res. Counc.* no. 376.

MEECHAM, W. C. & HURDLE, P. M. 1974 Use of cross-correlation measurements to investigate noise generating regions of a real jet engine and a model jet. *AGARD-CP*-131, paper 8.

MICHALKE, A. 1970 A wave model for sound generation in circular jets. *DLR-FB*, no. 70-57.

MICHALKE, A. 1971 New aspects of sound generation by circular jets. *Fluid Dyn. Trans.* **6**, 439–448.

MICHALKE, A. 1972 An expansion scheme for the noise from circular jets. *Z. Flugwiss.* **20**, 229–237.

MICHALKE, A. & FUCHS, H. V. 1974 Description of turbulence and noise of an axisymmetric shear flow. *DLR-FB*, no. 74-50.

MOLLO-CHRISTENSEN, E. 1963 Measurements of near-field pressure of subsonic jets. *AGARD Rep.* no. 449.

MOLLO-CHRISTENSEN, E., KOLPIN, M. A. & MARTUCCELLI, J. R. 1964 Experiments on jet flows and jet noise far-field spectra and directivity patterns. *J. Fluid Mech.* **18**, 285–301.

NAGAMATSU, H. T. & SHEER, R. E. 1972 Advanced fluid probe developments. *AFAPL-TR*-72-52, 612–716.

NAGAMATSU, H. T., SHEER, R. E. & BIGELOW, E. C. 1972 Mean and fluctuating velocity contours and acoustic characteristics of subsonic and supersonic jets. *A.I.A.A. Paper*, no. 72–157.

PAO, S. P. & LOWSON, M. V. 1968 Spectral technique in jet noise theory. *Wyle Res. Rep. WR* 68-21.

RIBNER, H. S. 1962 Aerodynamic sound from fluid dilatations. *University of Toronto, UTIA Rep.* no. 86.

SCHARTON, T. D. & WHITE, P. H. 1972 Simple pressure source model of jet noise. *J. Acoust. Soc. Am.* **52**, 399–412.

SCHARTON, T. D., WHITE, P. H. & RENTZ, P. E. 1973 Supersonic jet noise investigation using jet fluctuating pressure probes. *AFAPL-TR*-73-35.

SIDDON, T. E. 1969 On the response of pressure measuring instrumentation in unsteady flow. *University of Toronto, UTIAS Rep.* no. 136.